Targeting blood-brain barrier leakage for visualizing , monitoring, and evaluating ischemia reperfusion injury with Rus-Tc99m Probe

Shuaishuai Gong
China Pharmaceutical University
Jieman Wang
China Pharmaceutical University
Zhuo Chen
China Pharmaceutical University
Xuewei Pan
China Phaimaceutical University
Yunhao Wu
China Pharmaceutical University
Yuanyuan Zhang
China Pharmaceutical University
Boyang Yu
China Pharmaceutical University
Fang Li (lifangcpu@163.com)
China Pharmaceutical University
Junping Kou (junpingkou@cpu.edu.cn)
China Pharmaceutical University

Original research

Keywords: Ruscogenin, Technetium-99m, Blood-brain barrier, SPECT/CT, Ischemic reperfusion

Posted Date: May 6th, 2020

DOI: https://doi.org/10.21203/rs.3.rs-26295/v1

Abstract

Background : Cerebral ischemia-reperfusion (I/R) injury as a serious threat to human health is characterized by cerebral endothelial leakage, as a result of the damage of blood-brain barrier (BBB). It is thus quite attractive to realize real-time monitoring of BBB damage for therapeutic surveillance.

Methods : In this study, a radioactive probe is constructed by conjugating ruscogenin (Rus), a neuroprotectants, to technetium-99m (Tc 99m) to assess the damage of cerebral endothelial in BBB.

Results : In vitro study proves that the probe can penetrate more efficiently in damaged BBB. Then, longitudinal nuclear imaging distinguishes mice with BBB leakage from normal ones, which is validated by evans blue staining of brain tissue. Higher nuclear signal also correlates with poorer blood circulation in brain. Further, by visualizing brain signal during drug treatment, the probe finds that the most obvious protective efficacy of Rus occurs at 12 h post administration, which is superior than edaravone (Edara).

Conclusion : Altogether, the probe is promising to monitor I/R injury real-time by radioactive-imaging of BBB integrity. Importantly, Rus as a neuroprotectants may serve as a potential theranostic agent for I/R treatment.

Introduction

Ischemic stroke has become the number one cause of death in China, and it is a serious threat to human health. The clinical methods and drugs for treating ischemic stroke are very limited. To date, tissue-plasminogen activator (t-PA) is the only FDA-approved therapy for ischemic stroke. However, it usually exacerbates the disease through causing cerebral ischemia and reperfusion (I/R) injury[1–3]. I/R is characterized by a dynamic and complex pathophysiological process which preferably invade specific organs including heart, brain, kidney and intestinal[4]. Meanwhile, it is usually multiple and resistant to conventional therapies, hindering successful surgical resection and drug treatment, and remains a bottleneck for sensitive detection and effective treatment in clinic[5, 6]. As such, there is an urgent need to sensitively monitor the extent of damage to brain tissue by reperfusion and predict the development potential of stroke in the early stages. Therefore, it is particularly attractive to develop imaging methods with sufficient molecular information to assess the risk of brain injury. As a promising candidate, single photon emission computed tomography (SPECT) imaging can sensitively and accurately identify molecular classifications, avoiding optical quenchability and long-term instability. It is more convenient to use SPECT imaging for pharmacodynamic studies in animal models[7, 8] .

Abundant evidence has confirmed that the destruction of the blood-brain barrier (BBB) is the primary factor in the pathogenesis of I/R injury[9, 10]. Intravascular proteins and fluids penetrate into the extracellular space of the brain parenchyma, leading to vasogenic brain edema and reducing blood flow to neurons, leading to irreversible apoptosis[11, 12]. Some preclinical studies have proved that cerebral endothelial injury is the main sign of BBB destruction[13, 14]. Intensive investigation of the cerebral

endothelial is urgently needed. Previous studies have shown that ruscogenin (Rus) targets cerebral endothelial to inhibit NLRP3 activation and restrain NF-κB and ROCK/MLC pathways to improve I/R-induced BBB damage[15, 16]. Based on traditional pharmacokinetic analysis, the amount of Rus crossing the BBB is directly related to brain endothelium permeability. Such relatedness prompts that the method of cerebral endothelia-targeted Rus for both monitoring and evaluating drug efficacy could be developed, which is the motivation of exploiting novel image probe.

Technetium-99m (Tc^{99m}) has often been used to label radiopharmaceuticals, due to its suitable physical and chemical properties, along with reasonable radionuclide cost. This is an important characteristic of thermosensitive compounds since they may be degraded during the labeling process. Several chelating agents are currently used to prepare stable complexes with Tc^{99m}, including ethylenediamine diacetate (EDDA), which requires mild labeling conditions and fast reaction rates. Importantly, compound labeled with Tc^{99m} and chelating agents have negligible toxicity and demonstrate obvious merits in comparison with iodine-containing molecules[17]. The appropriate half-life of Tc^{99m} enables easy visualize to mornitor specific disease information for 24 h. In addition, SPECT combined with CT can be used as a structure and function detector for accurate assessment[18]. To date, the use of Tc^{99m} to target cerebral endothelial leakage for both damage imaging of BBB and drug efficacy assessments has rarely been reported.

In this study, an effective radioactive probe was developed using covalent conjugation of Tc^{99m} with Rus. Rus, is a major effective steroidal sapogenina in Chinese herb that has been applied to treat acute and chronic inflammatory and cardiovascular diseases for years. It has also been widely used to treat chronic venous insufficiency and vasculitis in Europe for decades due to its ability to decrease capillary permeability and anti-elastase activity[19, 20]. This probe (Rus-Tc^{99m}) is designed to identify, monitor and assess the extent of BBB leakage. OGD/R and MCAO/R mouse models have been used to confirm the permeability to different levels of brain endothelium in vitro and vivo. At the same time, the probe can be used to evaluate the drugs (ruscogenin and edaravone) efficacy on cerebral endothelial damage. Altogether, the probe is promising to evaluate I/R injury and evaluate drug efficacy in a real-time manner.

Methods

Animals and treatment

C57BL/6J mice weighing 18-22g were provided by the Reference Animal Research Centre of Yangzhou University (Yangzhou, People's Republic of China; certificate no SCXK 2014-0004). All procedures and assessments were approved by the Animal Ethics Committee of the School of Chinese Materia Medica, China Pharmaceutical University. These experiments were carried out in accordance with the National Institutes of Health Guide for the Care and use of Laboratory Animals (National Institutes of Health Publication No 80-23, revised in 1996). Before performing the experiments, all animals were randomized into experimental groups, and the indices were measured by operators blinded to the study procedures.

Middle cerebral artery occlusion(MCAO) model

A middle cerebral artery occlusion (MCAO) model was induced using the modified intraluminal filament method as follows: for blocking the blood supply to the ipsilateral hemisphere of the rat brain, the right middle cerebral artery was occluded by inserting a 4-0 nylon monofilament suture into the right internal carotid artery. The body temperature was sustained at 37℃ with a heated blanket throughout the procedure. The animals underwent 1h of MCAO and then were reperfused by careful withdrawal of the filament. In the sham group, an identical surgical procedure was performed without disturbing the arteries[21].

Oxygen and glucose deprivation/reperfusion(OGD/R)model

In order to generate I/R-like conditions by OGD/R in vitro, bEnd.3 cell was placed in a 37°C anaerobic chamber (0.2% O_2, 5% CO_2, 95% N_2) and cultured in glucose-free medium for 6h. After the oxygen-glucose deprivation, the cells were placed in glucose-containing DMEM with 10% FBS and then incubated under normoxic conditions for 24 h in order to affffect reperfusion. Control samples were taken from cells cultured under normal conditions[22].

Tracer synthesis

Rus was labeled with Tc^{99m} using tricine and EDDA as the coligands. The radiolabeling procedure was the literature method. In brief, to a clean vial were added 30 μL of a Rus solution (1 mg/mL in 30% ethanol), 200 μL of a tricine solution [100 mg/mL in 0.1 M phosphate buffffer (pH 6.0)], 25 μL of a $SnCl_2$ solution (1.0 mg/mL in 0.1 N HCl), and 100 μL of a $Na_2Tc^{99m}O_4$ solution (370 MBq) . The reaction mixture was kept at room temperature for 10 min. To the solution were added 500 μL of EDDA [20 mg/mL in 0.1 N HCl (pH 1.0)] and 250 μL of Na_2HPO_4 [0.2 M in H_2O (pH 8.5)]. The vial containing the reaction mixture was sealed, cramped, and heated at 60℃ for 40 min. After being cooled to room temperature, a sample of the resulting solution was analyzed by radio-HPLC with HPLC method. The structure is shown in Figure 1. The synthesis of Rus-Tc^{99m} and its radiolabeling were achieved as mentioned.

TTC staining

Brains were quickly removed at 12 h post-ischemia. The 2, 3, 5-triphenyl tetrazolium chloride (TTC) staining was performed to evaluate tissue viability and measure the infarct size. The infarct area was measured in NIH Image J software (Version 1.42; National Institutes of Health, Bethesda, Md). The infarct areas on each slice were summed and multiplied by slice thickness to give the infarct volume. Infarct volume was expressed as a percentage of infarction per ipsilateral hemisphere[23].

Millicell assay

Cells were incubated in the Millicell bEnd.3 cells culture inserts in a humidified atmosphere of 5% CO_2 and 95% air for 7d. After OGD/R condition, the medium was removed. 100 μL of EB & Rus-Tc^{99m} solution were added into the Millicell cell culture inserts and 1 mL of Krebs buffer were added into the external chamber.

The cells were continuously incubated for another 60 min and then the external Krebs solution were collected and added to 96-well black microplate. EB concentration value was measured at an excitation wavelength of 620 nm, with an emission wavelength of 530 nm using an Infinite M200 Pro plate reader (Tecan, NC, USA), radioactive counting value was measured by γ-ray counter.

Evans Blue (EB) in vivo

BBB permeability was assessed by the leakage of EB stain into the brain following the tail-vein injection. Two hours before the animals (n=6 for each group) were euthanized, 0.1 mL per 10 g body weight of 2% EB (Sigma Aldrich) in normal saline was injected into each animal. The animals were then anesthetized and perfused with normal saline. For the quantitative measurement of EB leakage, the ipsilateral hemisphere was removed and homogenized in 1 mL of trichloroacetic acid, then centrifuged at 12,000 g for 20 min. EB concentration was quantitatively determined by measuring the absorbance at 620 nm of the supernatant with a spectrophotometer. The EB content was quantified as micrograms of EB per gram of tissue, using a standard curve[24].

CBF measurement

Cerebral blood flow (CBF) was measured using laser Doppler flowmetry. A computer-controlled optical scanner directed a low-power laser beam over the exposed cortex. The scanner head was positioned parallel to the cerebral cortex at a distance of ~20 cm. A color-coded image indicating specific relative perfusion levels was displayed on a video monitor. The images were acquired at the onset of ischemia and reperfusion 0, 6, 12 and 24 h (n=6 for each group)[25].

Neurological deficits

Neurological deficits of the experimental animals were graded on an 18-point scale as previously described. The measurement of neurological deficits consisted of the following tests: spontaneous activity, symmetry of movements, symmetry of forelimbs, climbing, reaction to touch, and response to vibrissae touch. All six individual tests were scored on a four-point scale as 3, 2, 1, or 0. Final score was obtained by adding the scores recorded for each individual test, with a maximum score of 18 observed in healthy animals[26].

In vivo SPECT/CT

All in vivo imaging experiments were conducted on a dedicated small animal SPECT system (NanoSPECT/CT, Mediso) in Xiamen university, center for molecular imaging and translational medicine, calibrated for technetium-99m (Tc^{99m}) emitted γ-radiation. Tracers were applied in amounts, corresponding to 10 MBq/animal intravenously into the tail vein 24 h before in vivo imaging. The mean scan time was about 60 min with an initial morphologic whole body spiral CT and a consecutive whole body SPECT scan with a frame time of 60 s. Animals were held under Isoflurane inhalation anaesthesia (2% Isoflurane in air) for the whole scan time. Data were reconstructed and analysed using in built

VivoQuant Software and presented as percentage of the injected dose (%ID) per selected region of interest (ROI). For individual organ analysis, 3D ROIs were drawn on the anatomic CT images. The ROI size was identical for all parallel experiments. Mean values and standard deviation were calculated for %ID. After in vivo imaging, mice were either kept for longitudinal follow up examinations or sacrificed for tissue collection[7].

Western blot analysis

The cells or samples (n = 6, for each group) were decapitated and rapidly collected. The prepared cells or tissues were homogenized in 1:10 (w/v) ice-cold protein extraction buffer in glass homogenizers. Soluble proteins were collected and centrifuged at 12,000 g for 10 min at 4℃, and then the supernatant was used to detect the level of ZO-1, occludin and the total protein. The protein concentration of the samples was determined by BCA protein assay reagent kit. Equal amount of protein lysate (50 μg) in each group was separated by 8% and 12% sodium dodecyl sulfate-polyacrylamide gel electrophoresis (SDS-PAGE). The proteins on the gel were subsequently transferred onto a nitrocellulose membrane (260 mA, 2 h). The membranes were blocked with PBST containing 5% skim milk for 2 h at room temperature and then incubated with primary rabbit monoclonal antibody respectively overnight at 4℃(ZO-1, occludin, 1:800; Proteintech Group, USA). The membranes were then washed and incubated with secondary antibody (anti-rabbit IgG, 1:3000; Proteintech Group, USA) for 1.5 h at room temperature. The anti-actin antibody (1:1000; Proteintech Group, USA) served as control. The protein bands were visualized with enhanced chemiluminescence reagents (ECL), and the signal densitometry was quantified by an observer blinded to the groups of the animals using western blotting detection system (Quantity One, Bio-Rad Laboratories, USA)[28].

Statistical analysis

All results are expressed as mean±standard deviation (SD). GraphPad Prism (GraphPad software, San Diego, CA, USA) was used for statistical analysis of the data. The significant of the differences between two groups was analysed using unpaired Student's t test, and multiple comparisons was performed by one-way analysis of variance (ANOVA) followed by Dunnett's post hoc test. All tests were two-tailed. $P<0.05$ was considered statistically significant.

Results

The characterization of Rus-Tc^{99m}

The oxhydryl of Rus, Tricine, and the secondary amine of EDDA are coordination with the Tc^{99m}, which formed six coordination bonds. Rus-Tc^{99m} was synthesized and analyzed by HPLC. Due to the enhanced water solubility after the Tc^{99m} labeling, the peak time of Rus was delayed compared to the standard (Fig.1A-B).

In vitro targeting of Rus-Tc^{99m} probe to cerebral endothelial leakage

To determine the Rus-Tc^{99m} characterization in advance, we detected EB and radioactive counting extravastion in vitro. The millicell assay was used to construct different reperfusion time points, and the correlation between different degrees of barrier damage and EB, Rus-Tc^{99m} leakage was observed. The results showed that with extension of reperfusion time, the leakage rates of EB and the radioactive counting of Rus-Tc^{99m} increase, there is a linear relationship between the EB and Rus-Tc^{99m} (Fig.2A-E).

In vivo targeting of Rus-Tc^{99m} probe to BBB leakage

MCAO mouse models were constructed at different reperfusion time points, and the correlation between different degrees of barrier destruction and EB, Rus-Tc^{99m} leakage was observed using EB stain and SPECT imaging experiments. The results showed that with the prolongation of reperfusion time, the leakage rates of EB and Rus-Tc^{99m} significantly increased, and reached the highest point at 12 hours of reperfusion, there was a linear relationship between the EB and Rus-Tc^{99m} (Fig.3A-E). Meanwhile, the results shown in Fig. 3B demonstrated that Rus-Tc^{99m} generally were specifically delivered and distributed more in the brain, fewer in the lung, spleen and heart.

BBB leakage in accordance with blood flow in MCAO

In order to confirm the correlation between Rus and blood flow, Doppler flowmeter was used to detect blood flow changes at different reperfusion time points, SPECT imaging was used to detect the radioactive intensity of Rus-Tc^{99m} in real time. The results showed that as the reperfusion time prolonged, the blood flow became stable, but the intensity of Rus-Tc^{99m} radioactivity gradually increased and reached the highest level after 12 hours of reperfusion (Figure 4A, B). There was a negative correlation between blood flow and Rus-Tc^{99m} radioactivity (Figure 4C).

Evaluation efficacy based on SPECT imaging of BBB leakage

The above results showed that Rus-Tc^{99m} probe was able to detect the extent of BBB leakage. Then treated with Rus (10 mg/kg) and Edara to observe the correlation between Rus-Tc^{99m} and BBB. As is shown in Scheme 1, diagram of this part study. First, Rus was analyzed by HPLC in blood and in brain tissue (Supporting Fig.S1). After administration of Rus and Edara, EB stain and SPECT imaging were used to detect the leakage of BBB at different time points after reperfusion in vivo. The results showed that after the administration of Rus and Edara, the leakage rate of EB gradually decreased with the increase of reperfusion time, significant increase in CBF (Supporting Fig.S2) and the radioactive intensity of Rus-Tc^{99m} gradually weakened. The above results indicated that Rus and Edara could restore the integrity of BBB (Fig.5A-B). At the same time, it could be seen from the results that Rus exerted its effectiveness earlier than Edara in the reperfusion stage (Fig.5C-D).

Therapeutic effect of Rus on cerebral I/R injury

This study confirmed the effect of Rus on cerebral infarction volume, neurological score, ultrastructure of brain microvascular endothelial cell and the expression of tight junction protein (ZO-1, occludin) after 12 h of reperfusion in mice after cerebral ischemia. The results revealed that Rus obviously reduced the volume of cerebral infarction after cerebral ischemia for 1 h and reperfusion for 12 h (Fig.6A,B), which decreased the neurological score (Fig.6C). Besides, Rus also could increase the expression of ZO-1 and occludin (Fig.7A-B). However, Edara was less effective than Rus at 12h of reperfusion.

Discussion

Recent studies have shown the importance of the BBB in the development of stroke[30, 31]. BBB is a complex, multi-factor physiological environment. The BBB probe could detect the level of BBB permeability in real time, providing a basis for clinical monitoring of the development of stroke[32, 33]. Based on previous research, Rus could target cerebral endothelial to improve the BBB damage caused by I/R[15, 16]. Therefore, in this study, we chose Rus-Tc^{99m} as a probe for in vivo monitoring using SPECT imaging. Our current research provided direct evidence that Rus-Tc^{99m} depended on the permeability of BBB and targeted brain tissues. Administration of Rus could reduce the leakage rate of BBB and restore the expression of tight junctions. These results suggested that Rus might have potential as an adjuvant diagnosis and treatment to ischemic stroke.

In order to clarify the correlation between Rus-Tc^{99m} and barriers, this study first performed in vitro verification using small chamber EB and radiolabeling assay in vitro. The results showed that EB and radioactive intensity also differ with the increasing degrees of barrier permeability. The barrier permeability and leakage rate of EB raises the intensity of radioactivity also increased. Above results suggested that Rus-Tc^{99m} was positively related to the degree of barrier opening. In order to further explain the correlation between Rus-Tc^{99m} and the BBB, MCAO mouse models with varying degrees of BBB damage in vivo were constructed and confirmed by EB and SPECT imaging. The results showed that BBB permeability increased with prolonged reperfusion time, and radioactive intensity in the brain also increased with prolonged reperfusion time. In brief, the radioactive intensity of Rus-Tc^{99m} could represent the level of BBB permeability and play an important role in the clinical development of stroke.

Very importantly, we labeled Rus with Tc^{99m} to assess the damage of BBB in MCAO/R. Interestingly, Rus-Tc^{99m} accumulates in the ischemic hemisphere, which indicated that BBB was damaged during cerebral ischemia after reperfusion, and Rus might penetrate the ischemic brain tissue from the vascular space of the BBB. To further illustrate the correlation between the probe and the BBB, changes in blood flow were detected using a Doppler flowmeter. The results showed that although there was a negative correlation between the radioactive intensity in the brain tissue and the blood flow, they all indicated the level of BBB penetration. In other words, Rus-Tc99m Probe is promising to monitor I/R injury real-time by radioactive-imaging of BBB integrity. It was worth mentioning that Rus-Tc^{99m} didn’t rely on blood flow to enter brain tissue, but relied on the permeability of BBB to enter the lesion.

The above studies have all occurred under pathological conditions. In order to confirm the efficacy between Rus and Edara, this study administrated Rus-Tc^{99m} to observe the drug onset time in brain tissue during BBB recovery. EB results showed that Rus and Edara could restore the destruction of BBB, and SPECT imaging showed that during the BBB recovery, the radioactive intensity in the brain tissue gradually weakens. The above results indicated that the reduced permeability of BBB results in a reduction in the amount of Rus-Tc^{99m} entering the brain. Interestingly, it could be seen from the results that Rus exerted its effectiveness earlier than Edara's in 12 h after the reperfusion stage. Hence, Rus could intervene early in reperfusion injury, providing a guarantee for preventing further deterioration of the disease. Compared with Edara at 12 hours of reperfusion, Rus could significantly reduce the volume of cerebral infarction, recover the neurological score and repair tight junction as same as Fig. 6 and Fig. 7.

Our results indicate that Rus targets the cerebral endothelial cells and maintains the integrity of the BBB. Rus-Tc^{99m} Probe has a targeted recognition effect on the degree of BBB leakage in cerebral I/R injury. Our findings provide a novel strategy for the diagnosis and treatment of I/R stroke.

Conclusion

In this study, Rus-Tc^{99m} was developed with multiple capabilities to visualize, monitor and evaluate drug efficacy. The probe could accurately identify highly leaky cerebral endothelial and track their colonization in the brain by targeting the BBB. The molecular information revealed by Rus-Tc^{99m} provided an assessment of mouse BBB integrity. In particular, BBB damage increased with prolonged reperfusion, which explained the reason for the increased Rus-Tc^{99m} permeability. More importantly, we found that Rus targeted BBB to restore I/R-induced brain damage, while Rus-Tc^{99m} was able to evaluate the drug efficacy. Interestingly, the most obvious protective efficacy of Rus occurred at 12 h post administration, which was superior than Edara. The probe was promising to visualize and monitor I/R injury, accelerating that Rus would be applied in clinic.

Declarations

Ethics approval and consent to participate

All applicable international, national, and/or institutional guidelines for the care and use of animals were followed. All procedures performed in studies involving animals were in accordance with the ethical standards of the institution or practice at which the studies were conducted.

Consent for publication

Informed consent was obtained from all individual participants included in the study.

Availability of data and materials

Supporting information is available online.

Competing interests

All the authors declare no potential conflict of interest.

Funding

This research was supported by funding from the National Natural Science Foundation of the People's Republic of China (NO. 81773971), and the "Double First-Class" University project(CPU2018GF07).

Authors' contributions

Junping Kou conceived and directed this research; Shuaishuai Gong carried out SPECT/CT experiments and mouse stroke model studies; Jieman Wang and Zhuo Chen carried out cell culture based biological studies; Xuewei Pan and Yunhao Wu provided technical support for drug labling study; Yuanyuan Zhang contributed material for this project; Boyang Yu and Fang Li wrote the manuscript.

Acknowledgements

The authors thank the staff of the Key Laboratory of Natural Products, Jiangsu Key Laboratory of TCM Evaluation and Translational Research, China Pharmaceutical University for their valuable support.

Authors' information

Author name	Gender	Education	Email
Shuaishuai Gong	Male	Doctor	331864602@qq.com
Jieman Wang	Female	Master	1280223279@qq.com
Zhuo Chen	Male	Master	2116628171@qq.com
Xuewei Pan	Female	Master	441559233@qq.com
Yunhao Wu	Male	Doctor	834430875@qq.com
Yuanyuan Zhang	Female	Professor	15638392@qq.com
Boyang Yu	Male	Professor	395612293@qq.com
Fang Li	Female	Professor	lifangcpu@163.com
Junping Kou	Female	Professor	junpingkou@cpu.edu.cn

We are from State Key Laboratory of Natural Products, Jiangsu Key Laboratory of TCM Evaluation and Translational Research, Department of Pharmacology of Chinese Material Medical, College of Chinese Medicine, School of Traditional Pharmacy, China Pharmaceutical University, 639 Longmian Road, Nanjing, 211198, PR China

References

1. Valery LF, Grant N, Kelly C, Johnson CO, Alam T, Parmar PG, et al. Abate, Global, regional, and country-specific lifetime risks of stroke, 1990 and 2016. N Engl J Med. 2016;379:2429–37.
2. Chen WQ, Wang LH, Liu SW, Li YC, Wang LJ, Liu YN, et al. Cause-specific mortality for 240 causes in China during 1990–2013: a systematic subnational analysis for the Global Burden of Disease Study

2013. Lancet. 2016;387:251–72.
3. Catanese L, Tarsia J, Fisher M. Acute ischemic stroke therapy overview. Circ Res. 2017;127:541–58.
4. Chouchani ET, Pell VR, James AM, Work LM, Saeb-Parsy K, Frezza C, et al. A unifying mechanism for mitochondrial superoxide production during ischemia- reperfusion injury. Cell Metab. 2016;23:254–63.
5. Moskowitz MA, Lo EH, Iadecola C. The science of stroke: mechanisms in search of treatments. Neuron. 2010;67:181–98.
6. Saver JL, Fonarow GC, Smith EE, Reeves MJ, Grau-Sepulveda MV, Pan WQ, et al. Time to treatment with intravenous tissue plasminogen activator and outcome from acute ischemic stroke. JAMA. 2013;309:2480–8.
7. Eisenblaetter M, Flores-Borja F, Lee JJ, Wefers C, Smith H, Hueting R, et al. Visualization of tumor-immune interaction-target-specific imaging of S100A8/A9 reveals pre-metastatic niche establishment. Theranostics. 2017;7:2392–401.
8. Papadimitriou KI, Wang C, Rogers ML, Gowers SN, Leong CL, Boutelle MG, et al. High-performance bioinstrumentation for real-time neuroelectrochemical traumatic brain injury monitoring. Front Hum Neurosci. 2016;10:212.
9. Khatri R, McKinney AM, Swenson B, Janardhan V. Blood-brain barrier, reperfusion injury, and hemorrhagic transformation in acute ischemic stroke. Neurology. 2012;79:52–7.
10. Rodrigo R, Rodrigo FG, Rodrigo G, Matamala JM, Carrasco R, Miranda-Merchak A, et al. Oxidative stress and pathophysiology of ischemic stroke: novel therapeutic opportunities. CNS Neurol Disord Drug Targets. 2013;12:698–714.
11. Kou JP, Sun Y, Lin YW, Cheng ZH, Zheng W, Yu BY, et al. Anti-inflammatory activities of aqueous extract from Radix Ophiopogon japonicus and its two constituents. Biol Pharm Bull. 2005;28:1234–8.
12. Zheng Y, He RY, Wang P, Shi YJ, Zhao L, Liang J. Exosomes from LPS-stimulated macrophages induce neuroprotection and functional improvement after ischemic stroke by modulating microglial polarization. Biomater Sci. 2019;7:2037–49.
13. Vérité J, Janet T, Chassaing D, Fauconneau B, Rabeony H, Page G. Longitudinal chemokine profile expression in a blood-brain barrier model from Alzheimer transgenic versus wild-type mice. J Neuroinflammation. 2018;15:182.
14. Lochhead JJ, Ronaldson PT, Davis TP. Hypoxic stress and inflammatory pain disrupt blood-brain barrier tight junctions: implications for drug delivery to the central nervous system. AAPS J. 2017;19:910–20.
15. Guan T, Liu Q, Qian YS, Yang HP, Kong JM, Kou JP, et al. Ruscogenin reduces cerebral ischemic injury via NF-κB-mediated inflammatory pathway in the mouse model of experimental stroke. Eur J Pharmacol. 2013;714:303–11.
16. Cao GS, Jiang N, Hu Y, Zhang YY, Wang GY, Yin MZ, et al. Ruscogenin attenuates cerebral ischemia-induced blood-brain barrier dysfunction by suppressing TXNIP/NLRP3 inflammasome activation and

the MAPK pathway. Int J Mol Sci. 2016;17:9.

17. Holdy HT, Liu XD, Zou YD, Liu TA, Hu W, Chan H, et al. A novel peptide interfering with proBDNF-sortilin interaction alleviates chronic inflammatory pain. Theranostics. 2019;9:1651–65.
18. Pagkalos I, Rogers ML, Boutelle MG, Drakakis EM. A high-performance application specific integrated circuit for electrical and neurochemical traumatic brain injury monitoring. Chemphyschem. 2018;19:1215–25.
19. Bouskela E, Cyrino FZ, Marcelon G. Possible mechanisms for the inhibitory effect of Ruscus extract on increased microvascular permeability induced by histamine in hamster cheek pouch. J Cardiovasc Pharmacol. 1994;24:281–5.
20. Facino RM, Carini M, Stefani R, Aldini G, Saibene I. Anti-elastase and anti-hyaluronidase activities of saponins and sapogenins from Hedera helix, Aesculus hippocastanum, and Ruscus aculeatus: factors contributing to their efficacy in the treatment of venous insufficiency. Arch Pharm. 1995;328:720–4.
21. Zheng TT, Shi Y, Zhang J, Peng J, Zhang X, Chen KK, et al. MiR-130a exerts neuroprotective effects against ischemic stroke through PTEN/PI3K/AKT pathway. Biomed Pharmacother. 2019;117:109–17.
22. Li CR, Guan T, Chen XQ, Li WY, Cai QY, Niu QJ, et al. BNIP3 mediates pre-myelinating oligodendrocyte cell death in hypoxia and ischemia. J Neurochem. 2013;127:426–33.
23. Lan R, Xiang J, Wang GH, Li WW, Zhang W, Xu LL, et al. Xiao-Xu-Ming decoction protects against blood-brain barrier disruption and neurological injury Induced by cerebral ischemia and reperfusion in rats. Evid Based Complement Alternat Med. 2013; 2013: 629782.
24. Huang P, Zhou CM, Qin H, Liu YY, Hu BH, Chang X, et al. Cerebralcare Granule attenuates blood-brain barrier disruption after middle cerebral artery occlusion in rats. Exp Neurol. 2012;237:453–63.
25. Ahmad A, Genovese T, Impellizzeri D, Crupi R, Velardi E, Marino A, et al. Reduction of ischemic brain injury by administration of palmitoylethanolamide after transient middle cerebral artery occlusion in rats. Brain Res. 2012;147:45–58.
26. Jiang XY, Andjelkovic AV, Zhu L, Yang T, Bennett MV, Chen J, et al. Blood-brain barrier dysfunction and recovery after ischemic stroke. Prog Neurobiol. 2018; 144–171.
27. Kazuya K, Yuki I, Nobuhiko S, Nobuyoshi Umedab U, Laura F, Masafumi F, et al. On-site fabrication of Bi-layered adhesive mesenchymal stromal celldressings for the treatment of heart failure. Biomaterials. 2019;209:41–53.
28. Xu K, Xu C, Zhang YZ, Qi FR, Yu BR, Li P, et al. Identification of type IV collagen exposure as a molecular imaging target for early detection of thoracic aortic dissection. Theranostics. 2018;8:437–49.
29. Zhang S, Zhu D, Li H, Zhang H, Feng C, Zhang W. Analyses of mRNA profiling through RNA sequencing on a SAMP8 mouse model in response to Ginsennoside Rg1 and Rb1 treatment. Front Pharmacol. 2017;8:88.

30. Kelly PJ, Kavanagh E, Murphy S. Stroke: new developments and their application in clinical practice. Semin Neurol. 2016;36:317–23.
31. Mozaffarian D, Benjamin EJ, Go AS, Arnett DK, Blaha MJ, Cushman M, et al. Magid executive summary: heart disease and stroke statistics–2016 update: a report from the American heart association. Circulation. 2016;133:447–54.
32. Tobin MK, Bonds JA, Minshall RD, Pelligrino DA, Testai FD, Lazarov O. Neurogenesis and inflammation after ischemic stroke: what is known and where we go from here. J Cereb Blood Flow Metab. 2014;34:1573–84.
33. Giraud M, Cho TH, Nighoghossian N, Delphine MB, Deiana G, Østergaard L, et al. Early blood brain barrier changes in acute ischemic stroke: a sequential MRI study. J Neuroimaging. 2015;25:959–63.

Figures

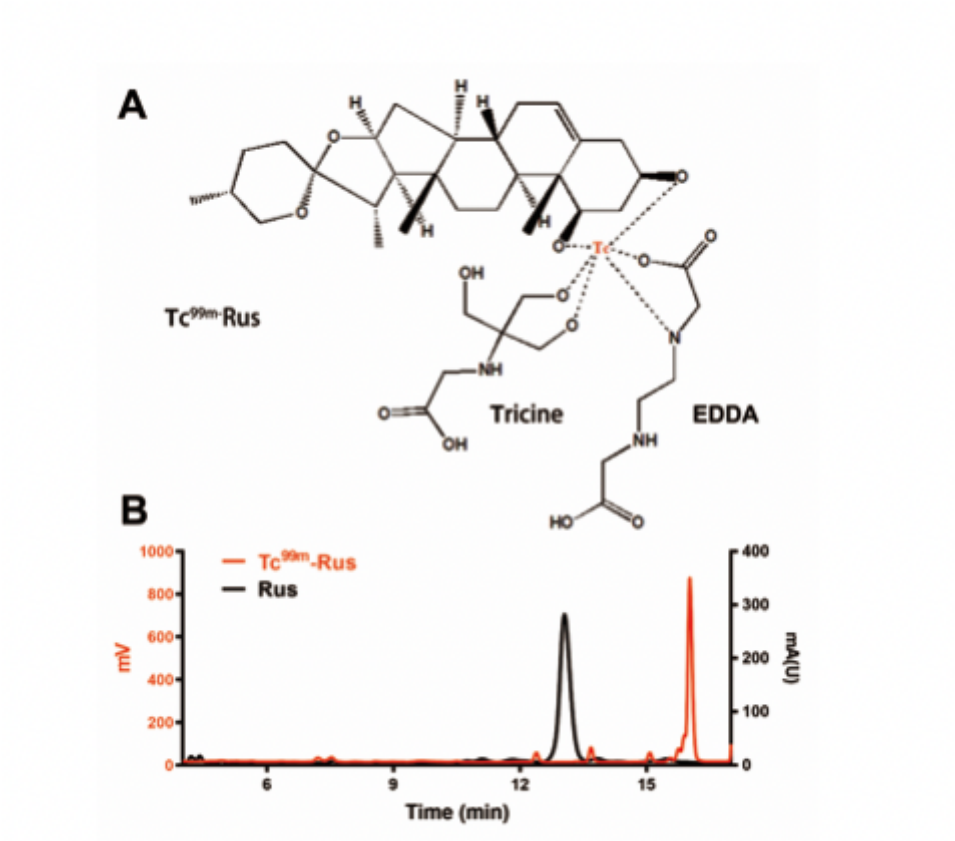

Figure 1

Preparation and characterization of Rus-Tc99m probe. A) Schematic illustration of the construction of the Rus-Tc99m probe. B) Rus-Tc99m was synthesized and analyzed by HPLC.

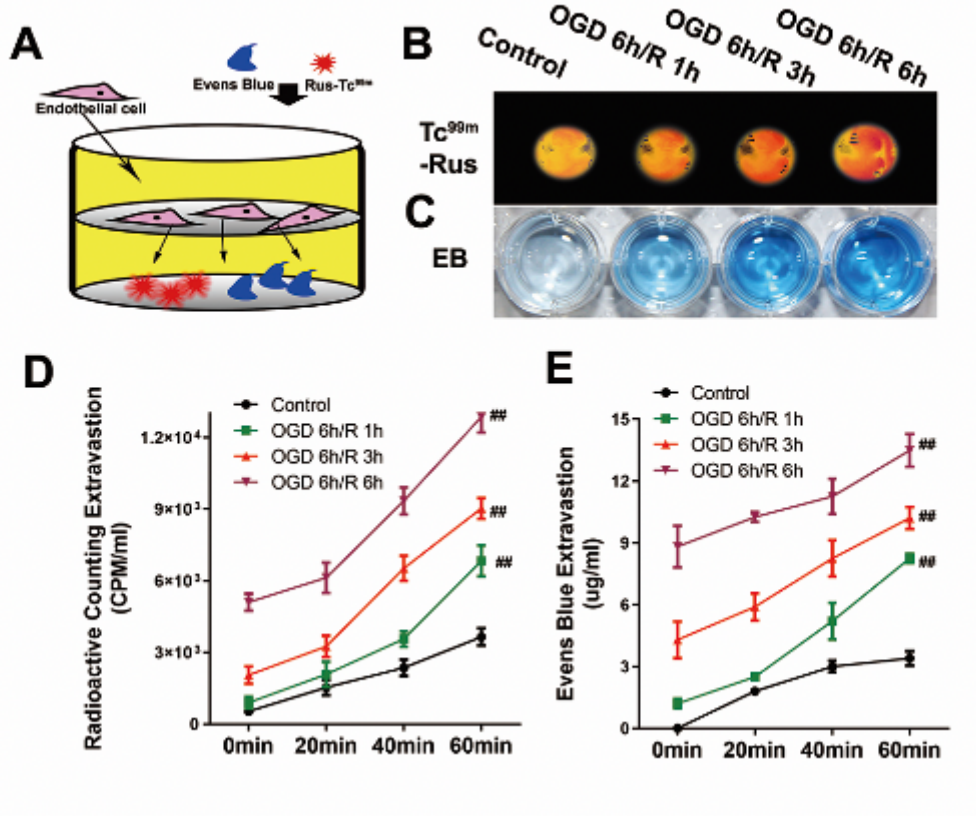

Figure 2

In vitro cerebral endothelial leakage with differently treatment. A)Schematic illustration of evens blue and autoradiography assay in vitro. B) Evens-blue leakage in vitro. C) Autoradiography detect radioactive intensity in vitro. D) Semiquantitative determination of the ratios of the radioactive intensity of lower layer. E) Semiquantitative determination of the evens blue extravastion of lower layer. Data were presented as mean±SD (n=3), ##P<0.01 vs control group; #P<0.05 vs control group.

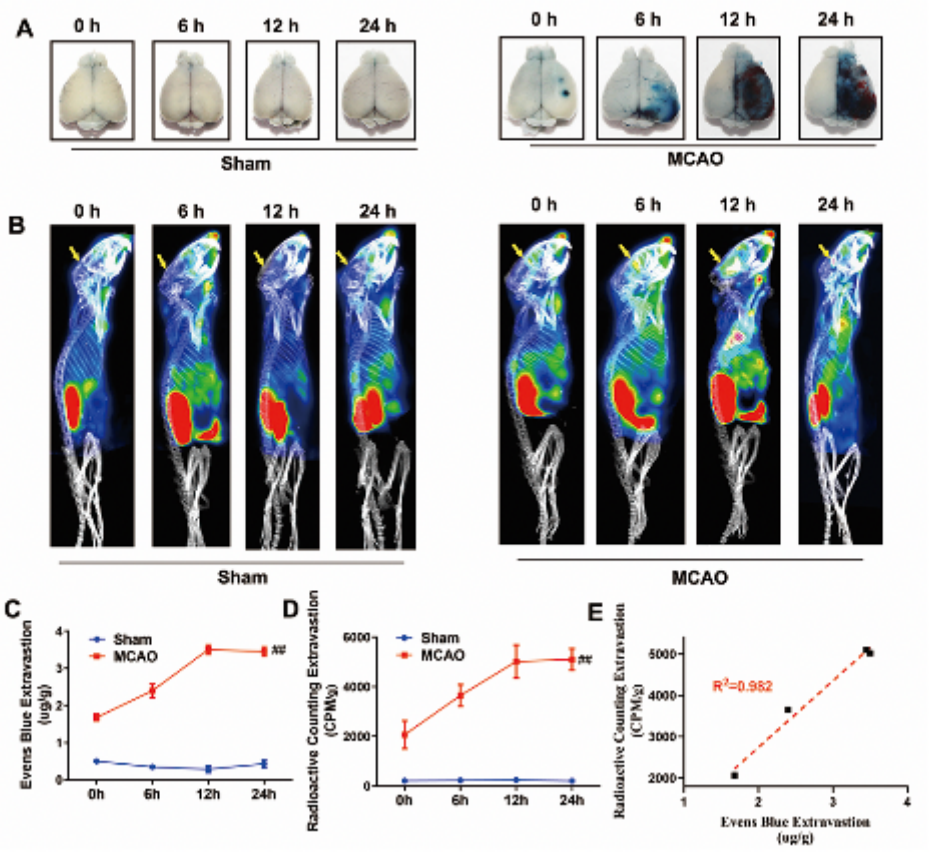

Figure 3

Detection of BBB leakage and blood flow in vivo with cerebral I/R. A) Evens-blue staining of the brain tissues from the mice. B) Using SPECT imaging to detect the distribution of Rus-Tc99m in vivo. C) Semiquantitative determination of the evens blue extravastion of brain. D) Semiquantitative determination of the ratios of the radioactive intensity of brain. E) Correlation between the evens blue extravastion and the ratios of the radioactive intensity. Data were presented as mean±SD (n=3), ##P<0.01 vs sham mice; #P<0.05 vs Sham mice

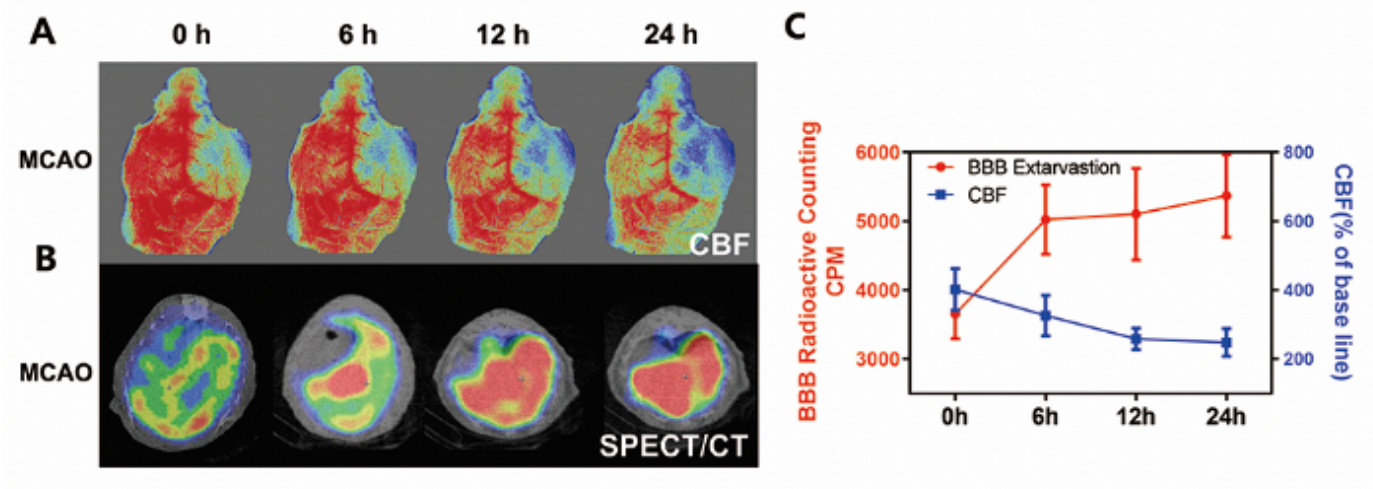

Figure 4

BBB leakage in accordance with blood flow A)The representative images of cerebral blood flow of ipsilateral cortex in MCAO/R group under different reperfusion time. The magnitude of CBF is represented by different colors, with blue to red denoting low to high. B) Using SPECT imaging to detect the distribution of Rus-Tc99m in brain. C) Semiquantitative determination of the ratios of the radioactive intensity (red line) and CBF (blue line) of brain. Data were presented as mean±SD (n=3).

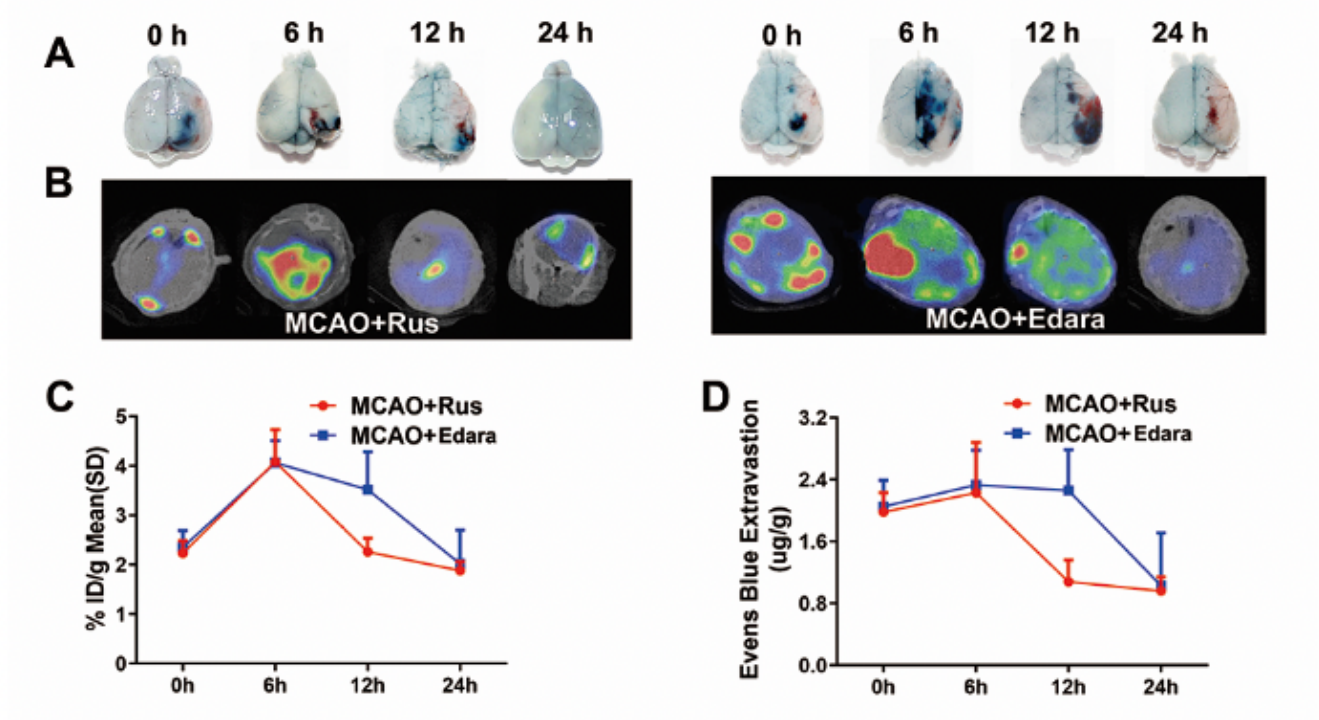

Figure 5

In vivo BBB leakage with differently treatment. A) Evens-blue staining of the brain tissues from the mice injected with differently drugs. B) In vivo imaging of the mice intravenously injected with differently treated using Rus-Tc99m. C) Semiquantitative determination of the ratios of the radioactive intensity of brain injected with differently drugs. D) Semiquantitative determination of the evens blue extravastion of brain injected with differently drugs. Data were presented as mean±SD (n=3).

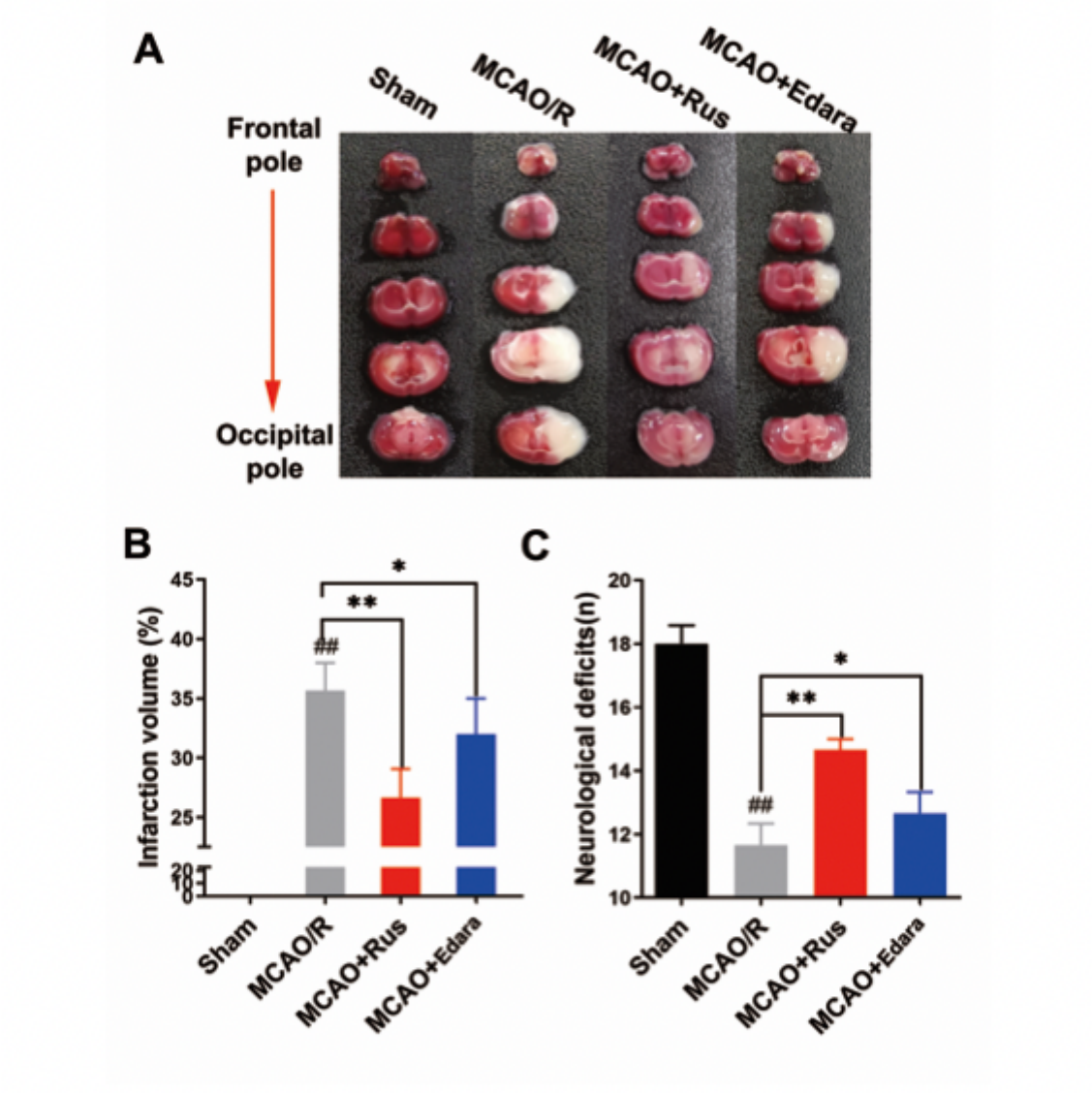

Figure 6

Therapeutic efficacy of Rus on cerebral I/R in mice. A, B) Infarct volume. C) Neurobehavioral outcomes. Data are expressed as mean±SD, n=6. ##P<0.01 vs sham mice; *P<0.05 vs I/R mice, **P<0.01 vs I/R mice.

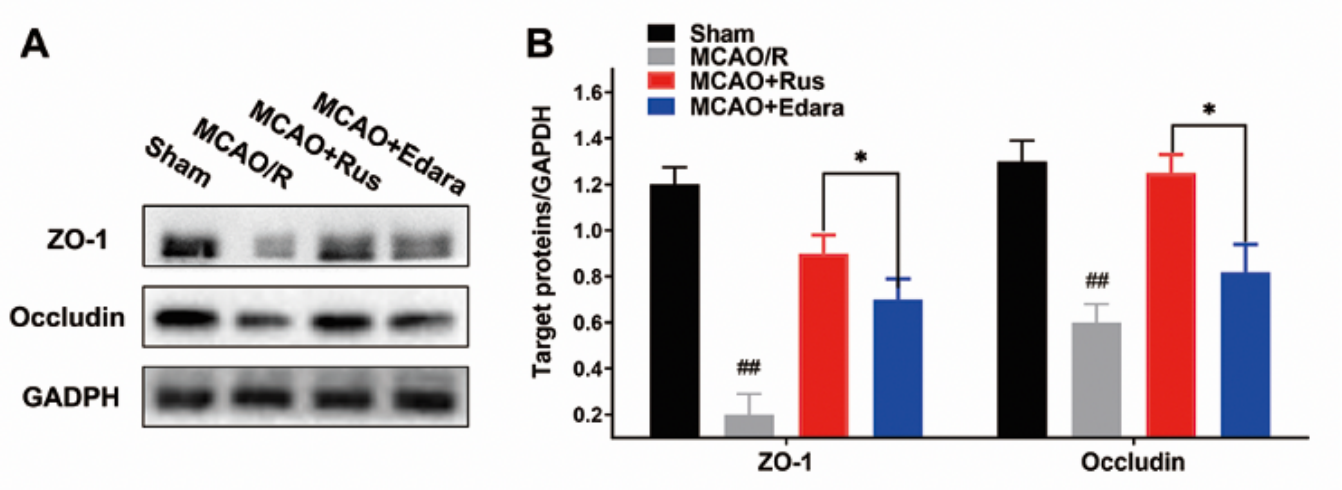

Figure 7

The expression of tight junction protein A) Expression of protein ZO-1, occludin in mice. Mice were subjected to 1 hour of ischemia and 12 hours of reperfusion. Rus was administered 1 hour after ischemia. Data are expressed as mean±SD, n=6. ##P<0.01 vs sham mice; *P<0.05 vs I/R mice, **P<0.01 vs I/R mice.

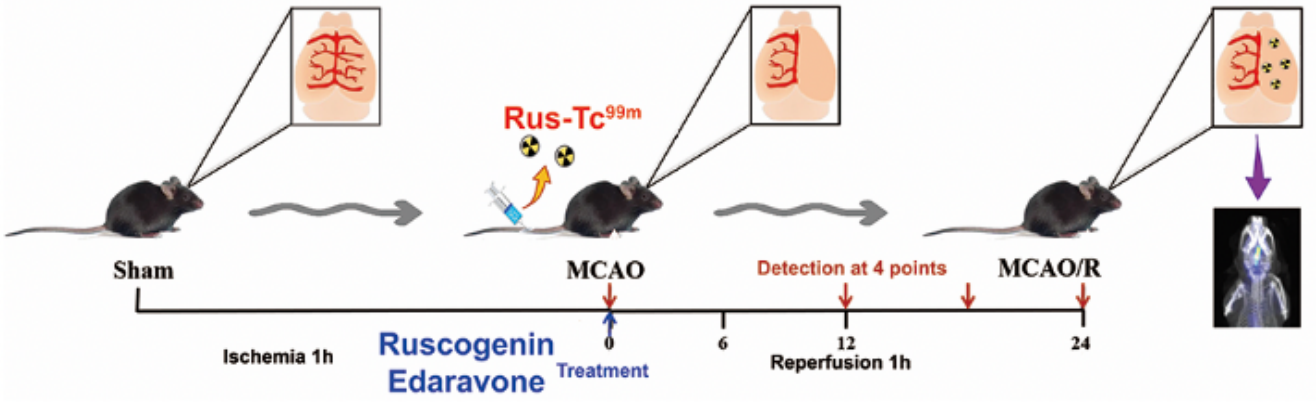

Figure 8

Scheme 1 Schematic illustration of the experiment procedure.

Supplementary Files

This is a list of supplementary files associated with this preprint. Click to download.

- Supplyment.docx